*13th IEA Heat Pump Conference 2020*


**13th IEA Heat Pump Conference**
April 26-29, 2021 Jeju, Korea

# Analysis of a steam generating high temperature heat pump for industrial waste heat recovery

Sabrina Dusek[a,*], Michael Lauermann[a], Franz Helminger[a], Veronika Wilk[a]

[a]AIT Austrian Institute of Technology GmbH, Giefinggasse 2, 1210 Vienna, Austria

**Abstract**

Steam is one of the most important energy carriers in industrial processes. For example, steam is used for sterilization, cooking and drying processes and as a heat transfer medium for various processes. Fossil fuels are often used to generate steam, but the use of fossil fuels, especially in industry, must be reduced in the future to reduce $CO_2$ emissions and to achieve climate targets. Heat pumps are already being used successfully in industrial applications, valorizing waste heat. With a high temperature heat pump, waste heat can be used to generate steam. This extension of the application range of heat pumps will provide a further contribution to achieving climate targets. A model of a steam generating high temperature heat pump was elaborated to study the technology under different operating conditions. This contribution shows the simulation results of a steam generating high temperature heat pump system with different refrigerants. The results are compared in terms of COP and compressor displacement. The goal is to identify the most appropriate refrigerant for a specific steam pressure.


Selection and/or peer-review under responsibility of the organizers of the 13th IEA Heat Pump Conference 2020.

*Keywords: High temperature heat pump; Industrial waste heat recovery; Steam generation; Modeling;*

## 1. Introduction

All over the world, industrial processes are rejecting large amounts of low temperature waste heat in the form of exhaust gases and waste water. According to an analysis of Forman et al [1], a total of 29 539 TWh of energy was supplied to industrial processes worldwide in 2012, but only 49% were actually used. The remaining 51% were identified as losses in the form of waste water and hot off gases (about two thirds of the losses) and other losses such as radiation, friction, resistance, etc. Due to the low temperature level, these waste heat streams can no longer be used in an efficient way and are released unused into the environment. High temperature heat pumps allow for using these waste heat streams because they provide process heat at a higher temperature level. Heat pumps that provide steam are of particular interest to the industry because steam generation has a significant share in process heat. For example, steam generation accounts for 27% of the useful energy in industry in Austria (92 PJ). A total of 45% of the steam was generated by combustion of natural gas (41 PJ). [2] If heat pumps are used for low pressure steam generation instead of steam generators operated with fossil fuels, significant reductions in primary energy and $CO_2$ emissions are achieved.

For steam production, high temperature heat pumps are required with supply temperatures up to 150°C, which are mainly determined by the choice of the refrigerant. Conventional industrial heat pumps can reach temperatures up to 90-100ºC, but new developments have raised the working temperature to above 100ºC in the last years (e.g. $CO_2$ based heat pumps from Engie Refrigeration [3] and Mayekawa (Japan) [4], R245fa heat pumps for the supply of hot water at 130°C by Ochsner Energietechnik GmbH (Austria) [5], heat pumps from Viking Heat Engines AS (Norway) with supply temperatures above 150ºC).

* Corresponding author. Tel.: +43-664-825-1411; fax: +43-505-506-679.
*E-mail address:* Sabrina.Dusek@ait.ac.at.

**Nomenclature**

*Abbreviations*

| | |
|---|---|
| COP | coefficient of performance |
| GWP | global warming potential |
| NBP | boiling point at nominal pressure |
| ODP | ozone depletion potential |
| SPHE | shell and plate heat exchanger |

*Roman symbols*

| | |
|---|---|
| a | pattern amplitude, m |
| A | heat transfer area, $m^2$ |
| d | plate diameter, m |
| h | specific enthalpy, $Jkg^{-1}$ |
| h" | specific enthalpy of dry saturated steam, $Jkg^{-1}$ |
| m | mass, kg |
| $\dot{m}$ | mass flow, $kgs^{-1}$ |
| n | number of plates |
| l | length of the plate pack, m |
| p | pressure, $bar_a$ |
| $P_{el}$ | electrical power, W |
| $\dot{Q}_H$ | heating capacity, W |
| $\dot{Q}$ | heat flow, W |
| s | plate thickness, m |
| t | time, s |
| V | volume, $m^3$ |
| X | wave number |

*Greek symbols*

| | |
|---|---|
| $\Lambda_P$ | wave length, m |
| $\Phi$ | area extension factor |

*Subscripts*

| | |
|---|---|
| in | incoming |
| out | outgoing |

Heat pumps for steam generation are still very rarely used in industrial processes. A 200 kW pilot plant was integrated into the Smurfit Kappa Roermond paper mill in the Netherlands by TNO (former ECN), which proved the ability to deliver steam at 120°C from a waste heat source at 60°C with R600 (critical temperature 152°C) as refrigerant. Based on the results of this project a roadmap for industrial heat pumps was created. [6-7] In 2011, a heat pump with R245fa was launched on the Japanese market under the brand name Kobelco, which supplies steam at 120°C and has a heating capacity of around 370 kW. The critical temperature of R245fa is 154°C. To achieve higher steam temperatures of 165°C, a vapour compressor can be connected downstream (SGH 165) [8]. Recently, Kaida published an overview on industrial applications of SGH heat pumps in Japan, reporting end user satisfaction and positive effects of the heat pump integration. The heat pump steam generators are applied in the chemical industry for distillation of ethanol (5 units supplying 2t/h of 120°C steam), sterilization of chemical containers (1 unit, 165°C steam) and for sewage sludge drying (1 unit, 165°C steam). [9] Those heat pumps are currently only available in Japan.

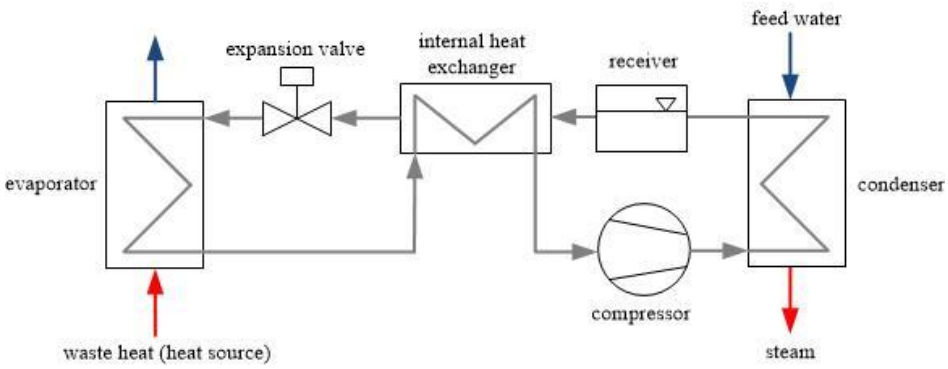


Fig. 1. Schematic representation of the steam generating heat pump cycle

In the BAMBOO project, the prototype of a heat pump is developed, which provides low-pressure steam with up to 5 $bar_a$ (152°C) for industrial steam networks. A novel HFO-refrigerant, R1336mzz(Z) is applied that has no negative impact on the environment. It is well suited for high supply temperatures of up to 160°C, thus for the production of saturated steam at up to 5 $bar_a$. A novel type of piston compresssor is selected as the compressor, which is already operating successfully on R1336mzz(Z). An innovative condenser is developed, where steam is generated directly on the secondary side. Thereby the heat pump becomes more efficient, compact and cost-effective. The heat pump prototype has a nominal heating capacity of 200 kW and can be easily scaled up to higher heating capacities. The heat pump will be thoroughly tested in the lab and then implemented in real industrial environment to demonstrate functionality at TRL7.

All the above-mentioned examples for steam generating heat pumps are subcritical processes. Subcritical processes are well suited for steam generation because the majority of heat is transferred at constant temperature. In this work a simulation model for a subcritical steam generating heat pump cycle is discussed. Fig. 1 illustrates the layout of the heat pump cycle. A shell and plate heat exchanger (SPHE) is used as the condenser and it is also the steam generator. The simulation model was used to compare different refrigerants, in terms of coefficient of performance (COP) and compressor displacement, using the same heat pump cycle. The analysis was carried out for three different steam pressures. The aim of this investigation was to find the most suitable refrigerant for a specific steam pressure.

## 2. Steam generating heat pump model

The steam generating heat pump cycle was modeled in the simulation environment Dymola/Modelica [10]. The TIL-Library [11] was used to model the components in the cycle. For the evaporator, the internal heat exchanger, receiver and the expansion valve standard components from this library were used. The condenser and the compressor were modeled in a custom way. The models of the individual components are described in more detail in the following chapters. A receiver after the condenser (see Fig. 1) enables the lowest possible condensation temperature for a wide range of operating conditions. For determining the required thermal-physical properties of the involved media (Refrigerants, Water) the TILMedia-Library [11] was used. Both thermal and pressure losses were neglected in this model. In addition, constant values were assumed for the heat transfer coefficients between the media and the heat transfer area of the heat exchangers.

### *2.1. Shell and Plate heat exchanger model*

As mentioned before, in the steam generating heat pump a SPHE is used as condenser. This particular type of heat exchanger is a combination of a shell and tube and a plate heat exchanger [12]. In this heat exchanger arrangement, the rounded corrugated plate pack is surrounded by a cylindrical shell filled with the secondary fluid as it is shown in Fig. 2. The plate pack is welded so that the primary and secondary fluid streams flowing through the channels do not come into contact. [12–14] The welded construction has the advantage that significantly higher operating temperatures and pressure levels are possible [13-14]. However, the disadvantage is the limited accessibility which makes cleaning more difficult [14].

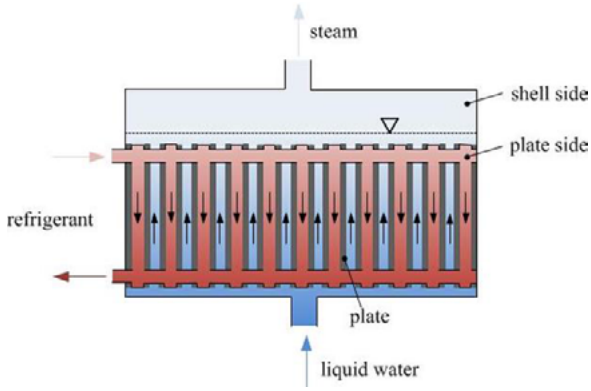


Fig. 2. Schematic representation of the modelled plate-and-shell heat exchanger

In the steam generating heat pump the steam is produced with the SPHE, therefore the shell side of the heat exchanger contains a two-phase fluid of liquid water and steam. The condensing refrigerant is located at the plate side (see Fig. 2). The following assumptions for modelling the SPHE were made:

- Heat exchange between the refrigerant and the water was entirely done via the plates
- Only the vertical flow of the refrigerant between the plates was considered
- In each refrigerant channel the same mass flow with the same temperature enters
- In each refrigerant channel the same mass flow with the same temperature exits
- Thermodynamic equilibrium between the two water phases on the shell side
- Plates are not contact with the steam phase

The length of the plate pack l, which is equal to the length of the cylindrical shell was calculated as shown in equation (1), where the number of plates n, the plate thickness s and the pattern amplitude a are needed.

$$l = (n-1) \cdot 2a + n \cdot s \tag{1}$$

The heat transfer area A between water and refrigerant can be calculate with equation (2).

$$A = (n-2)\frac{d^2}{4}\pi \cdot \Phi \tag{2}$$

The calculation of the area extension factor Φ (equation (3)), which occurs in equation (2), was done as it is presented in the VDI Heat Atlas [15]. The area extension factor describes the ratio between the wavy plate surface and the plane surface projection. For the calculation a sinusoidal corrugation of the plates was assumed. For the calculation of the area extension factor the wave number X is needed, which depends on the plate amplitude and the wavelength $\Lambda_P$ (equation (4)).

$$\Phi = \frac{1}{6}\left(1 + \sqrt{1+X^2} + 4\sqrt{1+\frac{X^2}{2}}\right) \tag{3}$$

$$X = \frac{2\pi a}{\Lambda_P} \tag{4}$$

In Fig. 2 horizontal feedthroughs of the refrigerant, which are arranged at the plate side of the SHPE, are shown, which reduce the surface area. This reduction is neglected in equation (2). The shell side contains a two-phase fluid of liquid water and steam. The incoming mass flow of liquid water $\dot{m}_{in}$ enters the liquid water

volume and the outgoing steam mass flow $\dot{m}_{out}$ exits the steam volume. A thermodynamic equilibrium between the two phases is assumed. Therefore, only one energy and mass balance equation according to equation (5) and equation (6) must be fulfilled. Both phases on the shell side have the same pressure and are connected by an evaporating mass and energy flow. The evaporating mass flow has the specific enthalpy of dry saturated steam.

$$\frac{dm}{dt} = \dot{m}_{in} + \dot{m}_{out} \tag{5}$$

$$m\frac{dh}{dt} = \dot{m}_{in}(h_{in} - h) + \dot{m}_{out}(h_{out} - h) + \dot{Q} + V\frac{dp}{dt} \tag{6}$$

*2.2. Plate heat exchanger model*

For modeling the internal heat exchanger and the evaporator, the standard plate heat exchanger model from TIL-Library was used. This model is based on the geometry of the heat exchanger described by the number of plates, length and width of the plate and other properties, and two heat transferring fluids. In addition to that, the heat transfer model and pressure drop model can be chosen for both heat transferring fluids separately. Different correlations to describe the heat transfer and the pressure drop are available. In order to describe the heat conduction mechanism within the plate, it can be chosen as a constant heat resistance value or the heat conduction is calculated based on the given plate geometry and material. In this work the geometry based method was used.

*2.3. Compressor and expansion valve model*

In order to reduce the complexity of the steam generating heat pump model, the compressor was modelled based on isentropic and volumetric efficiency instead of using a physical approach as in the positive displacement compressor model from the TIL-Library. Therefore, the efficiencies are given as a function of pressure ratio. Furthermore, an electrical efficiency must be defined in the model. The pressure difference between discharge and suction side are given by the evaporator and the condenser model. Therefore, the electric power is calculated in the compressor model with a given swept volume and the actual efficiencies.

For the expansion valve an orifice valve component based on the equation of Bernoulli from the TIL-Library was used. An effective flow area of the valve must be given in this component.

**3. Numerical simulations**

The aim of the investigation was to assess the suitability of different refrigerants for three different steam pressures provided by the steam generating heat pump. Table 1 presents the properties of the considered refrigerants in terms of critical temperature, critical pressure, global warming potential (GWP), ozone depletion potential (ODP) and boiling point at nominal pressure (NBP).

The refrigerants listed in Table 1 are not all suitable for each studied steam pressure. Therefore, Fig. 3 illustrates the estimated possible steam temperatures for each of the selected refrigerants. Moreover, the saturation temperature for each studied pressure is shown by the vertical dashed lines. The diagram starts at 100°C, because this is equal to the saturation temperature for steam at atmospheric pressure. Only subcritical processes are considered in this work, therefore the upper limit is defined based on the critical temperature of the refrigerant and the assumption of a minimum temperature difference between refrigerant and steam temperature of 10 K. R601, R601a and R1336mzz(Z) are suitable for all steam pressures. R1233zd(E) and R1224yd(Z) are suitable for 2 and 4 $bar_a$ steam. R600, R1234ze(Z) and R600a can only be used for 2 $bar_a$ steam.

Table 1. Properties of the used refrigerants

| Refrigerant | Critical temperature, °C | Critical pressure, bara | GWP | ODP | NBP °C | Reference |
|---|---|---|---|---|---|---|
| R601 | 196.6 | 33.7 | 5 | 0 | 36.1 | [16] |
| R601a | 187.3 | 33.8 | 5 | 0 | 27.9 | [17-18] |
| R1336mzz(Z) | 171.3 | 29 | 2 | 0 | 33.4 | [16] |
| R1233zd(E) | 166.5 | 36.2 | 1 | 0.00034 | 18 | [16] |
| R1224yd(Z) | 155.5 | 33.3 | <1 | 0.00012 | 14 | [16] |
| R600 | 152 | 38 | 4 | 0 | -0.5 | [16] |
| R1234ZE(Z) | 150.1 | 35.3 | <1 | 0 | 9.8 | [16] |
| R600a | 134.7 | 36.3 | 3 | 0 | -11.8 | [16] |

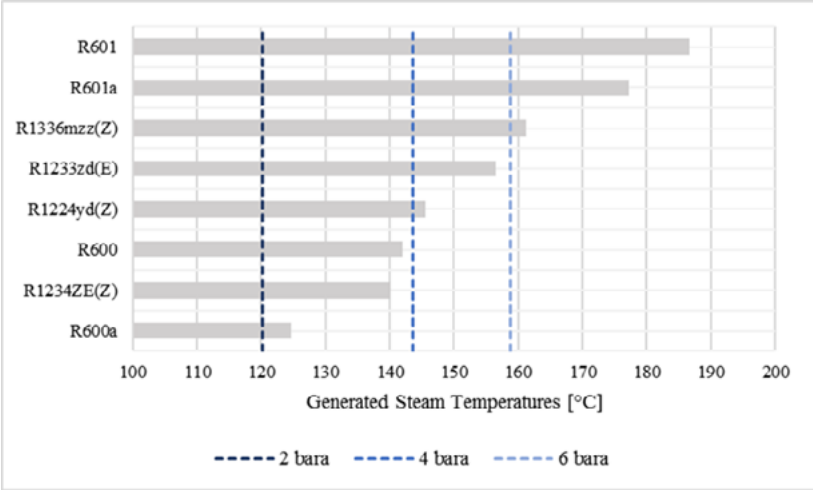


Fig. 3. Possible generated steam temperatures for the used refrigerants

### *3.1. Boundary conditions and control strategy*

For all refrigerants and steam pressures the same model settings were used for geometry, heat transfer coefficients, liquid feed water temperature (85°C), heat source temperature (85°C) and generated steam mass flow (200kgh$^{-1}$). Only the heat transfer area of the internal heat exchanger has been adapted to achieve a superheating of approximately 15 K after the compressor, which is exemplarily shown in the log(p), h-diagram of R601 in Fig. 4.

Moreover, the mass flow of the source fluid was controlled in such a way that the heat source will be cooled down by 5 K in the evaporator, under the restriction of a heat source mass flow higher than 0.4 t/h. The expansion valve is regulated so that saturated vapour is present at the outlet of the evaporator. The compressor displacement is controlled according to the desired steam pressure at the outlet of the condenser, it is equal to the pressure on the shell side of the SPHE. The liquid feed water mass flow is set to a constant value for the filling level in the SPHE. The liquid filling level is the ratio between the liquid water volume and the total shell side volume of the SPHE. It is assumed that the plate pack of the SPHE is only in contact with the liquid water phase for the chosen liquid filling level. All the control mechanisms explained before are realized as continuous control with PI controllers from the TIL-Library.

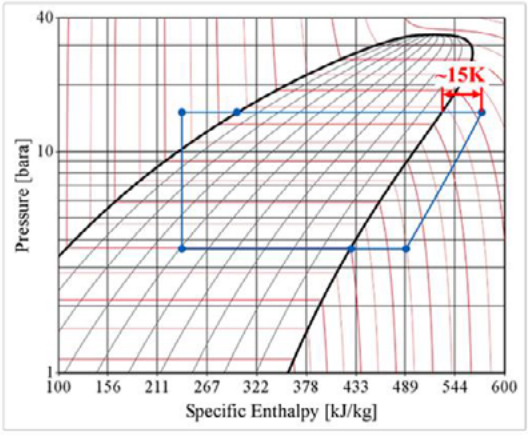


Fig. 4. Log(p), h diagram of R601 and refrigeration cycle for 4 bara generated steam pressure

*3.2. Results*

The different refrigerants are compared in terms of COP and compressor displacement, the corresponding results are shown in Fig. 5 and Fig. 6. The COP is calculated as it is presented in equation (9), where the heating capacity $\dot{Q}_H$ and the electrical power of the compressor $P_{el}$ are needed.

$$COP = \frac{\dot{Q}_H}{P_{el}} \tag{9}$$

If 2 $bar_a$ steam is produced, the COP is in the range of 3.26 and 4.3. For a steam pressure of 4 $bar_a$ the COP is in the range of 2.28 and 2.89. A COP in the range of 1.93 and 2.29 is reached for a steam pressure of 6 $bar_a$. R601 has the highest critical temperature and provides the highest COP for all steam pressures (see Fig. 5).

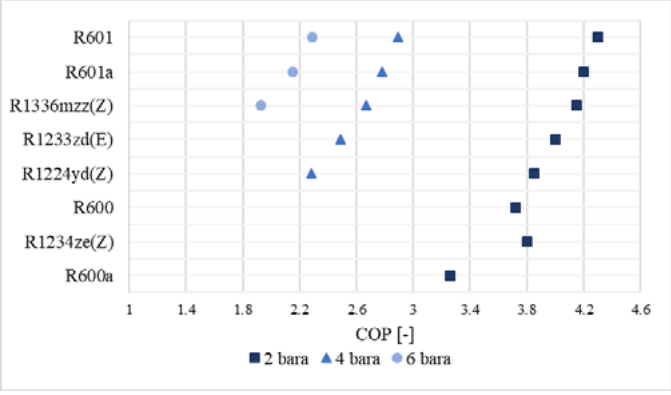


Fig. 5. COP for different refrigerants and steam pressures

The choice of refrigerant influences the COP to large extent. For example, using R1233zd(E) instead of R1224yd(Z) for a steam pressure of 4 $bar_a$ results in an increase in COP of 9%. Comparing R600a and R601 for the production of 2 $bar_a$ steam, the difference in COP amounts to about 24%. These differences can hardly be overcome only by adjusting the design of the refrigeration cycle.

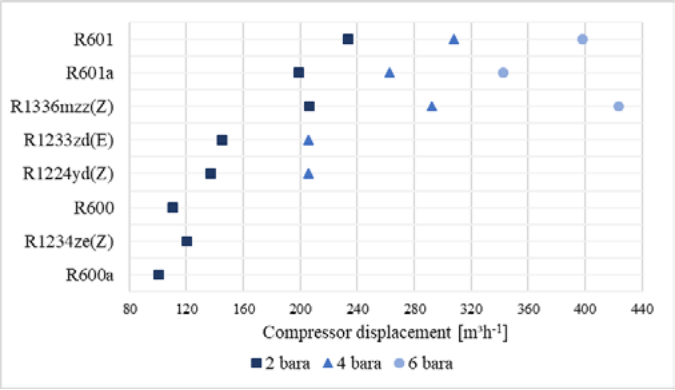


Fig. 6. Compressor displacement for different refrigerants and stem pressures

Furthermore, the results in terms of compressor displacement (Fig. 6) shows that R601 has the highest compressor displacement for all steam pressures except at a steam pressure of 6 $bar_a$. For this steam pressure the compressor displacement of R1336mzz(Z) is higher than for R601. In Fig. 5 it can be seen that the COP significantly decreases for higher steam pressures and the compressor displacement increases more or less with increasing steam pressure as it can be seen in Fig. 6.

Generally, it is easy to see that the choice of refrigerant is a trade-off between COP and compressor displacement, which leads to larger compressors. For example, for a steam pressure of 2 $bar_a$ the COP of R1233zd(E) is 7% smaller than the COP of R601, but the compressor displacement of R1233zd(E) is 38% smaller than the compressor displacement of R601. This leads to a significant smaller compressor, where the COP is not decreasing that significantly. For the steam pressure of 6 $bar_a$ R1336mzz(Z) shows the lowest COP but the highest compressor displacement.

In Fig. 7 the condensation enthalpy as a function of suction gas density for a steam pressure of 2 $bar_a$ and all tested refrigerants are presented. The condensation enthalpy is equal to the width of the two-phase area in loq(p),h-diagram at condensation pressure. As it can be seen, R601 and R601a have the highest condensation enthalpy but also the lowest suction gas density. The high COP of R601 can among others be explained by the high condensation enthalpy. For R600 and R1336mzz(Z) the suction gas density is similar, but the condensation enthalpy of R600 is significantly higher than that of R1336mzz(Z). The suction gas densities of R600a and R1233zd(E) and the condensation enthalpies are very similar to each other. Fig. 7 illustrates the differences in material properties of the refrigerants, that have an important impact on the performance in a heat pump.

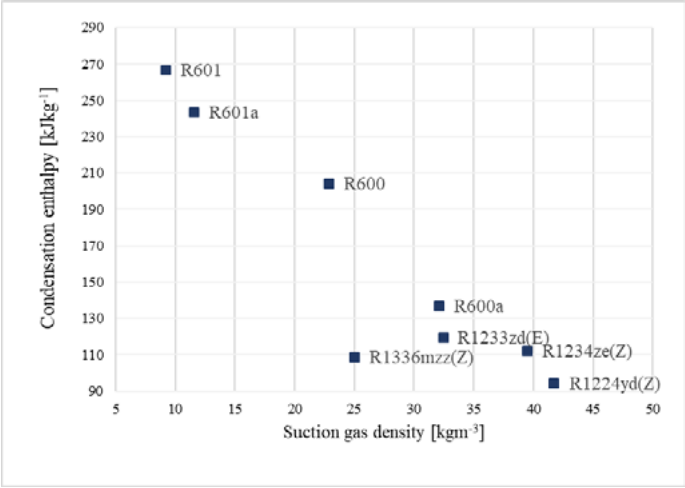


Fig. 7. Condensation enthalpy as a function of suction gas density for all investigated refrigerants and a steam pressure of 2 $bar_a$

## 4. Conclusion

In this work a model for a steam generating heat pump is presented. Simulations are an important tool for the design of heat pump systems and help to optimize the refrigeration cycle in an efficient way. This model was used for studying the suitability of different refrigerants for different generated steam pressures in a specified steam generating heat pump. The investigation has proven that the model is well suited to design the steam generating heat pump for different applications or requirements.

Furthermore, the simulation results show for the different preselected refrigerants and steam pressures, a range of 1.93-4.3 in terms of COP and a range of 101-424 $m^3h^{-1}$ in terms of compressor displacement. R601 has the highest COP of 4.3, 2.89 and 2.29 for the three chosen steam pressures of 2 $bar_a$, 4 $bar_a$ and 6 $bar_a$. This refrigerant shows also the highest compressor displacement for a steam pressure of 2 $bar_a$ and 4 $bar_a$, which results in the largest required compressor volume. The choice of refrigerant is a trade-off between COP and compressor displacement. The choice of refrigerant also has an important influence on both investment and operation cost. The COP mainly determines the operation costs, the compressor displacement is an indicator of the size of the heat pump and therefore impacts on the investment costs. However, when selecting the refrigerant for a real implementation, attention must be paid to the fact that market-ready components are not available for all refrigerants. For example, R1336mzz(Z) and R600 are refrigerants which are already used in heat pump cycles and therefore all components are available. In contrast to R600, which is only suitable for a steam pressure of 2 $bar_a$, R1336mzz(Z) is suitable for all three investigated steam pressures. Therefore, in the project BAMBOO R1336mzz(Z) is used in the refrigeration cycle to generate steam at 5 $bar_a$. In the next step a prototype will be realized in the project BAMBOO which will be tested in a laboratory environment as well as in a real industrial process. Moreover, different heat pump cycle configurations and further operating conditions will be investigated in future investigations.

As an outlook for future technological developments, it should not go unmentioned that further industrial users can be gained by expanding the range of available industrial heat pumps. The investment decisions of industrial users are ultimately influenced by economic aspects. Therefore, optimized design of the industrial heat pumps and the use of standard components to lower the costs are important. Current technical limitations, such as maximum possible steam pressures, should be overcome by further efforts.

**Acknowledgements**

The project has received funding from the European Union's Horizon 2020 programme for energy efficiency and innovation action under grant agreement No. 820771.

**References**

[1] Forman C, Muritala I K, Pardemann R, and Meyer B. Estimating the global waste heat potential. *Renewable and Sustainable Energy Reviews* 2016; **57**: 1568–1579.
[2] Statistik Austria, STATcube- Statistical database of Statistik Austria. Useful energy analysis 2016 (in German), accessed on March 23 2018.
[3] ENGIE Refrigeration GmbH, $CO_2$-chillers and $CO_2$-high temperature heat pumps (in German). https://www.engie-refrigeration.de/export/sites/cofelyrefrigeration/content/documents/DE/Broschueren/thermeco2/DE_Folder_thermeco_W%C3%A4rmepumpen_web.pdf, accessed on October 29 2019.
[4] Davis T W. Introduction of Mayekawa's ECO cute water source hot water heat pump at Torres De Alba Hotel: Using the Natural Refrigerant $CO_2$. In*: Atmosphere America Business Case Natural Refrigerants* 2014, June 18-19, San Francisco, http://www.atmo.org/presentations/files/460_4_Mayekawa_Davis.pdf, accessed on January 01 2020.
[5] OCHSNER Energie Technik GmbH, Highest temperature series (IWWDS, ISWDS, IWWDSS) (in German), http://ochsner-energietechnik.com/hoechsttemperatur-waermepumpen/, accessed on October 29 2019.
[6] Wemmers A K, Van Haasteren A W M B, Kremers P, Van der Kamp J. Test results R600 pilot heat pump. In: *12th IEA Heat Pump Conference 2017*, May 15-18, Rotterdam, Netherlands.
[7] De Boer R. Industrial heat pumps in the Netherlands-developments and demonstrations. In: Zühlsdorf B, Bantle M, Elmegaard B, editors. *Book of presentations of the 2nd Symposium on High-Temperature Heat Pumps* 2019, September 09, Copenhagen, Denmark.
[8] Kaida T, Sakuraba I, Hashimoto K, Hasegawa H. Experimental performance evaluation of heat pump-based steam supply system . *IOP Conference Series: Materials Science and Engineering* 2015; **90**: 012076.
[9] Kaida T. High-temperature heat pumps in Japan- Potential, development trends and case studies. In: Zühlsdorf B, Bantle M, Elmegaard B, editors. *Book of presentations of the 2nd Symposium on High-Temperature Heat Pumps* 2019, September 09, Copenhagen, Denmark.
[10] Dassault Systèmes, https://www.3ds.com/de/produkte-und-services/catia/produkte/dymola/, accessed on November 01 2019.
[11] TLK-Thermo GmbH, https://www.tlk-thermo.com, accessed on November 01 2019.
[12] Ayub ZH. Plate heat exchanger literature survey and new heat transfer and pressure drop correlations for refrigerant evaporators. *Heat Transfer Engineering* 2003; **24**(5): 3–16,.
[13] Arsenyeva OP, Tovazhnyanskyy LL, Kapustenko PO, Khavin GL, Yuzbashyan AP, Arsenyev PY. Two types of welded plate heat exchangers for efficient heat recovery in industry. *Applied Thermal Engineering* 2016; **105**: 763–773.
[14] Lim J, Song KS, Kim D, Lee DC, and Kim Y. Condensation heat transfer characteristics of R245fa in a shell and plate heat exchanger for high-temperature heat pumps. *International Journal of Heat and Mass Transfer* 2018; **127**(A): 730–739.
[15] *VDI Heat Atlas*. VDI-Gesellschaft Verfahrenstechnik und Chemieingenieurwesen, editor. Springer-Verlag Berlin Heidelberg 2010, 2nd edition, Germany.
[16] Arpagaus C. *High temperature heat pumps: Market overview, state of the art and potential applications* (in German). VDE Verlag GmbH 2019, Berlin, Germany.
[17] Umweltbundesamt. Global Warming Potential (Global Warmin Potential, GWP) of selected compounds and their mixtures according to IPCC Fourth Assessment Report over a period of 100 years (in German), https://www.umweltbundesamt.de/sites/default/files/medien/2503/dokumente/treibhauspotentiale_ausgewaehlter_verbindungen_und_deren_gemische.pdf, accessed on November 01 2019.
[18] Ge Z, Li J, Duan Y, Yang Z, Xie Z. Thermodynamic performance analyses and optimization of dual-loop organic rankine cycles for internal combustion engine waste heat recovery. *Applied Sciences* 2019; **9**(4):680.